Scheraga, H. A. (1963) *Proteins, 2nd Ed. 1*, 545-546.
Schimerlik, M. I., & Cleland, W. W. (1977a) *Biochemistry 16*, 565-570.
Schimerlik, M. I., & Cleland, W. W. (1977b) *Biochemistry 16*, 576-583.
Schimerlik, M. I., Grimshaw, C. E., & Cleland, W. W. (1977) *Biochemistry 16*, 571-576.
Silverberg, M., & Dalziel, K. (1975) *Methods Enzymol. 41*, 214-220.
Tang, C. L., & Hsu, R. Y. (1974) *J. Biol. Chem. 249*, 3916-3922.
Tomkins, G. M., Yielding, K. L., & Curran, J. F. (1962) *J. Biol. Chem. 237*, 1704-1708.
Velick, S. F., Baggott, J. P., & Sturtevant, J. M. (1971) *Biochemistry 10*, 779-786.
Weder, H. G., Schildnecht, J., Lutz, R. A., & Kesselring, P. (1974) *Eur. J. Biochem. 42*, 475-481.
Welcher, F. J. (1958) *Analytical Uses of Ethylenediaminetetraacetic Acid*, pp 1-17, Van Nostrand, New York.
Winer, A. D. (1964) *J. Biol. Chem. 239*, 3598-3600.
Winer, A. D., Schwert, G. W., & Miller, D. B. S. (1959) *J. Biol. Chem. 234*, 1149-1154.

Kinetic Studies of the Malic Enzyme of Pigeon Liver. "Half-of-the-Sites" Behavior of the Enzyme Tetramer in Catalysis and Substrate Inhibition†

Robert Y. Hsu* and Terry A. Pry‡

ABSTRACT: A steady-state analysis is carried out at pH 7.0 to determine the kinetic significance of the two types of Mn^{2+} and malate binding sites on malic enzyme, detectable by direct binding studies [Pry, T. A., & Hsu, R. Y. (1980) *Biochemistry* (preceding paper in this issue)]. At saturating $NADP^+$, malate exhibits Michaelis-Menten behavior, with K_A (Mn^{2+}) of 8.5-33 μM and K_M (malate) of 47-63 μM, corresponding to the binding of these reactants at two "tight" metal [$K_D \simeq 8$ μM; Hsu, R. Y., Mildvan, A. S., Chang, G. G., & Fung, C. H. (1976) *J. Biol. Chem. 251*, 6574-6583] and substrate ($K_D \simeq 23$-30 μM) sites. Saturation of Mn^{2+} at "weak" metal sites ($K_D \simeq 0.9$ mM) has no effect on the catalytic rate. High (but physiological) levels of malate cause uncompetitive substrate inhibition vs. [Mn^{2+}], at low Mn^{2+} concentrations occupying only the tight metal sites. The apparent K_i of malate is 182-270 μM, which corresponds to the binding of malate at two remaining weak sites ($K_D \simeq 250$-400 μM). High concentrations of Mn^{2+} relieve malate inhibition with a K_A' of $\simeq 0.64$ mM, as the result of binding at weak metal sites. A "half-of-the-sites" model is proposed which shows that only two of the four putatively identical subunits of this enzyme simultaneously undergo catalysis. The catalytic rate is inhibited by malate through binding at the adjacent low-affinity sites, and the inhibition is overcome by binding of Mn^{2+} at the same sites. Malate also inhibits the Mg^{2+}-activated reaction. Under in vivo conditions, malic enzyme probably exists in the partially inhibited form, subject to regulation by changes in the levels of malate and the metal activator.

Previous EPR studies (Hsu et al., 1976) have shown that malic enzyme of pigeon liver binds the activating metal Mn^{2+} at two high-affinity sites and two to four low-affinity sites. In the preceding paper of this series, we reported equilibrium binding studies on $NADP^+$, NADPH, the substrate malate, and the inhibitor oxalate. The nucleotides bind independently and equivalently to the putatively identical subunits of the enzyme tetramer. Malate binding is promoted by Mn^{2+} and NADPH in accordance with an ordered kinetic mechanism with malate binding last in the reaction sequence. As with Mn^{2+}, malate binds to two types of sites with differing affinity. "Half-of-the-sites" reactivity is shown by the inhibitor oxalate which binds firmly to only two of the available sites. Mn^{2+} shows kinetic negative cooperativity at inhibitory levels of malate, and the double-reciprocal velocity vs. [Mn^{2+}] plots concave downward with increasing Mn^{2+} concentration. This paper presents a more detailed steady-state kinetic study using $NADP^+$ concentration saturating the four available sites and Mn^{2+} and malate concentrations saturating the two high-affinity sites or both high- and low-affinity sites. The unusual kinetic and binding behavior of this enzyme uncovered in these studies is interpreted in terms of a half-of-the-sites model whereby only two of the four enzyme sites are simultaneously undergoing catalysis. A preliminary report of this work has been published (Hsu & Pry, 1979).

Experimental Section

Materials

TEA-HCl (A grade),[1] EDTA, Tris-HCl (enzyme grade), and DTT (Calbiochem), L-malic acid (Schwarz/Mann), $NADP^+$ (P-L Biochemicals), Sephadex G-200 (Pharmacia), Dowex 1-X10 (Mallinckrodt), DE-52 (Whatman), and $MnCl_2$ (Fischer Scientific) were purchased from the above sources. Distilled, deionized water was used throughout this work. The nucleotide solutions were made up fresh daily.

Methods

The preparation of pigeon liver malic enzyme and enzyme assays were performed as described in the preceding paper (Pry & Hsu, 1980). One unit of enzyme activity is defined as the amount which catalyzes the conversion of 1 μmol of substrate per min under the conditions of the assay. The kinetic assays

† From the Department of Biochemistry, State University of New York, Upstate Medical Center, Syracuse, New York 13210. *Received August 9, 1979.* Supported in part by grants from the National Institutes of Health (AM 13390 and 5507RR05402). This research is derived from the dissertation of T.A.P. presented in partial fulfillment for the requirements of a Ph.D. degree.

‡ Present address: Lipid Metabolism Laboratory, Veteran's Administration Hospital, Madison, WI 53705.

[1] Abbreviations used: TEA-HCl, triethanolamine hydrochloride; Tris, tris(hydroxymethyl)aminomethane; DTT, dithiothreitol.

0006-2960/80/0419-0962$01.00/0

Table I: Kinetic Parameters[a] of Malic Enzyme Catalyzed Oxidative Decarboxylation

fixed substrate:	Mn^{2+} (10–100 μM)	malate (5–50 μM)	malate (5 μM–15 mM)							
variable substrate:	malate (5–50 μM)	Mn^{2+} (10–100 μM)	Mn^{2+} (10 μM–10 mM)							
kinetic constants:	K_m[c]	K_A[c]	K_m[d]	K_i[d]	K_A[e]	$\bar{V}_m$[d]	K_A'[e]	$\bar{V}'_m$[e]	K_A'[f]	$\bar{V}'_m$[f]
preparation 1[b]	52	16	63	270	10	59	480	48	399	33
preparation 2[b]	55	33	47	182	8.5	30.8	800	21	2730	20.3

[a] K_m is the Michaelis constant of malate and K_i is the apparent inhibition constant of malate with Mn^{2+} saturating K_A. $\bar{V}_m$ and $\bar{V}'_m$ are the maximum uninhibited and deinhibited velocities, respectively. K_A and K_A' are the two sets of activator constants for Mn^{2+}. The kinetic constants are expressed in μM except for $\bar{V}_m$ and $\bar{V}'_m$ which are given in terms of micromoles of NADPH formed per minute per milligram of enzyme. [b] Preparation 1 represents the fully active enzyme whereas preparation 2 represents a partially aged enzyme with some loss of activity. [c] Obtained from Figure 1. [d] Obtained from Figure 3. [e] Obtained from Figure 2A (K_A) and Figure 2B (K_A' and $\bar{V}'_m$). [f] Obtained from Figure 2C.

were performed essentially as described above except that the reactions were carried out at pH 7.0 in TEA-HCl buffer, 150 μmol; the $MnCl_2$ additions were from 0.03 to 90 μmol and the malate additions were from 0.015 to 45 μmol.

A tetrameric molecular weight of 260 000 and a subunit molecular weight of 65 000 were used for malic enzyme (Nevaldine et al., 1974) in all calculations. Commercial malate was purified through a Dowex 1-X10 column according to Pry & Hsu (1980).

Data Analysis. The nomenclature used in this paper is that of Cleland (1963a). Data conforming to a sequential initial velocity pattern, linear uncompetitive inhibition, and linear competitive inhibition were fitted to the appropriate equations as described previously (Hsu et al., 1967). The fitting was carried out by the least-squares method assuming equal variance for the velocities (Wilkinson, 1961). All least-squares fits reported here were performed by a digital computer and the FORTRAN programs of Cleland (1963b). The points in the double-reciprocal plots are the experimentally determined values while the lines drawn through these points are calculated from the fits of these data to the appropriate rate equations.

Results

Inhibition by Malate. The inhibition of Mn^{2+}-activated oxidative decarboxylase activity by high malate concentrations (≥0.3 mM) and the reversal of this inhibition at high $MnCl_2$ concentrations (≥0.1 mM) have been observed in previous kinetic studies (Hsu et al., 1976; Schimerlik et al., 1977). More recently, stopped-flow kinetic studies (Reynolds et al., 1978) indicated that malate inhibits the reaction by forming an abortive E–Mn^{2+}–NADPH–malate complex, from which NADPH dissociates at a rate slower than from the E–NADPH complex formed at noninhibiting malate concentrations. However, the detailed mechanism of this process appears to be complex, involving both nonequivalence of substrate and metal binding sites and interactions between adjacent subunits of the enzyme tetramer. In the current work, the kinetic behavior of Mn^{2+} and malate was reinvestigated in order to assess the functional significance of the heterogeneous classes of binding sites.

Figure 1 shows plots of $1/v$ vs. reciprocal total Mn^{2+} at fixed levels of noninhibitory malate concentrations (5–50 μM). The $MnCl_2$ concentration was varied 1000-fold (10 μM–10 mM) to affect binding at the two "tight" ($K_D \simeq 8$ μM) and two to four "weak" ($K_D \simeq 0.9$ mM) metal sites (Hsu et al., 1976). In these experiments, data points at high $MnCl_2$ concentrations (1 and 10 mM) were obtained by preadjusting the amount of malate in each cuvette to a higher level to compensate for the significant decrease in free (active) malate concentration due to formation of Mn^{2+}–malate chelate. The plots converged on the horizontal axis as seen previously (Hsu et al., 1976).

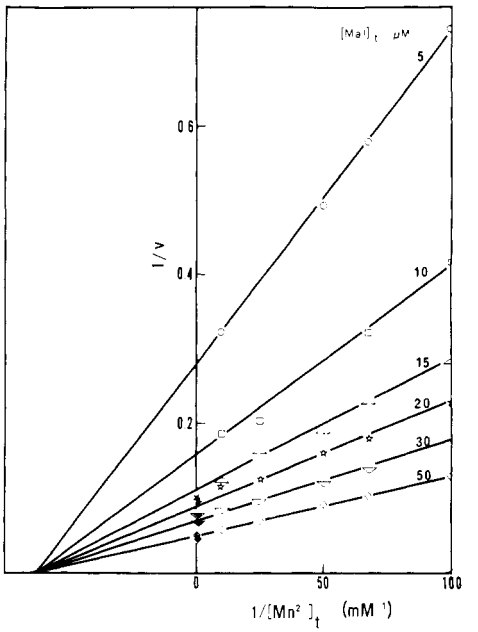

FIGURE 1: Double-reciprocal plots with Mn^{2+} as the variable component at noninhibitory malate concentrations. The kinetic assays for oxidative decarboxylase activity were performed at pH 7.0, 30 °C, as described under Methods, at saturating (217 μM) $NADP^+$ and variable levels of malate and $MnCl_2$. Malate concentrations at low $MnCl_2$ (≤100 μM, open symbols) were uncorrected for the Mn^{2+}–malate complex. At higher $MnCl_2$ (1 mM, closed symbols) and 10 mM (cross hatched symbols), significant amounts of chelation complex were formed. These data points were obtained at malate concentrations preadjusted for the formation of the chelation complex (K_D = 20 mM; Hsu et al., 1976) to give the desired malate level ($[Mal]_f$) in uncomplexed form. The data were taken from experiments using malic enzyme preparation 1. The velocities are expressed in micromoles of NADPH formed per minute per milligram of enzyme.

Significantly, the reciprocal velocity plots yielded typical Michaelian patterns for Mn^{2+}, which did not deviate from linearity even at high Mn^{2+} concentrations known to result in heterogeneous binding of this activator at the weak as well as tight metal sites. From these plots, a K_A (activation constant for Mn^{2+}) of 16 μM (average 24 μM for two enzyme preparations, Table I) was obtained.

Replotting of the results in Figure 1 as $1/v$ vs. $1/[malate]$, at different levels of Mn^{2+}, yielded a similar intersecting pattern and a Michaelis constant of malate (K_m) of 52 μM (average 53 μM for two enzyme preparations, Table I).

Double-reciprocal plots obtained at inhibitory levels of malate are shown in Figure 2A. In these experiments, the malate concentrations were increased >1000-fold from 5 μM to 7 mM, at a wide range of $MnCl_2$. Clearly, substrate inhibition was apparent at low levels (≤20 μM) of the activator.

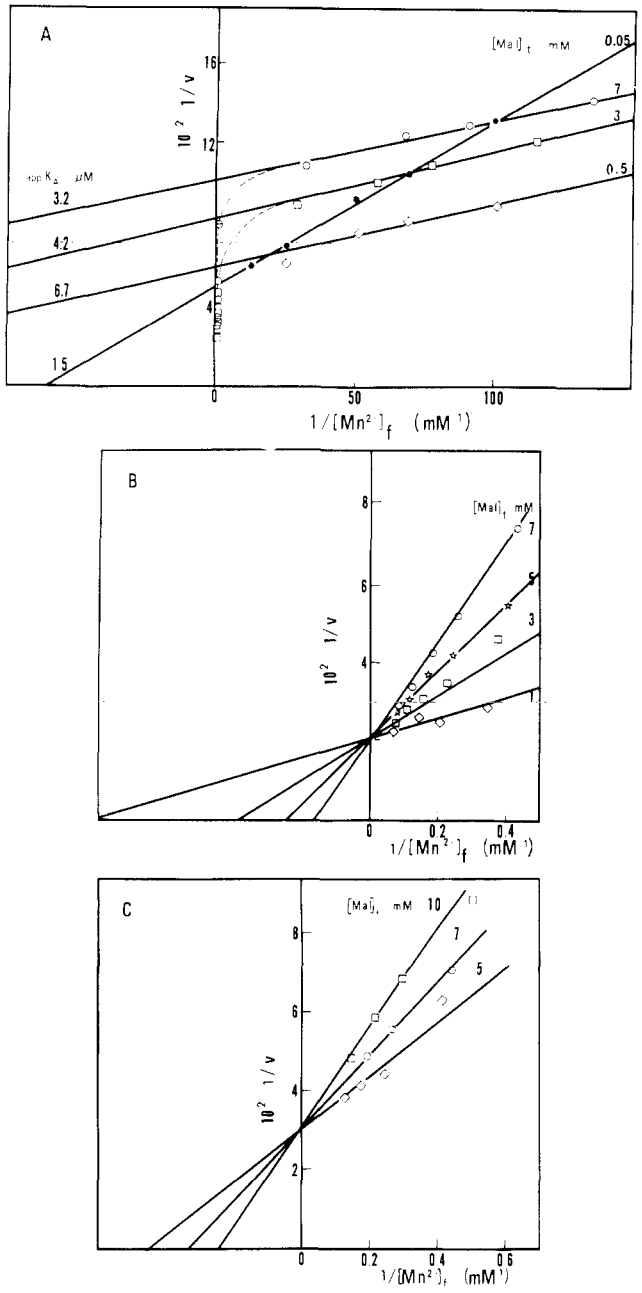

FIGURE 2: Double-reciprocal plots with Mn^{2+} as the variable component at inhibitory levels of malate. The kinetic assays were performed as indicated in Figure 1 using malic enzyme preparation 1, except that a wide range of malate, including high (inhibitory) concentrations, was used. (A) Double-reciprocal plots of $1/v$ vs. $1/[Mn^{2+}]$ at fixed levels of malate. The $MnCl_2$ and malate concentrations were 10 μM–10 mM and 5 μM–7 mM, respectively. The experiment (up to 99 determinations) was performed in a single day. The stability of malic enzyme was indicated by complete recovery of activity at the end of the experiment as determined by oxidative decarboxylase assays. For the purpose of clarity, only data points for one noninhibitory (50 μM) and three inhibitory (0.5, 3, and 7 mM) levels of malate were shown. At malate concentrations of 0.5 mM and above, the Mn^{2+} concentrations were expressed as $[Mn^{2+}]_f$ after correcting for the Mn^{2+}–malate complex (K_D = 20 mM; Hsu et al., 1976). (B) Enlarged view of plots at high Mn^{2+} concentrations. (C) Enlarged view of plots as in (B) from a separate experiment where data points were obtained at malate concentrations preadjusted for the formation of the Mn^{2+}–malate chelation complex as in Figure 1.

Increasing Mn^{2+} caused apparent activation and downward curvature of the plots, however, only at inhibitory malate concentrations (cf. Figure 1). The uncompetitive inhibition pattern (solid lines) is consistent with the ordered binding of Mn^{2+} and malate (Cleland, 1970). The latter inhibits NADPH release by forming an abortive E–Mn^{2+}–NADPH–malate complex (Reynolds et al., 1978) with fractional occupancy of Mn^{2+} at the tight metal sites; additional binding of the metal reverses this inhibition.

The following experiment was carried out to ascertain that inhibition was induced by the substrate and not by a contaminant in the commercial malate preparation. For this purpose, L-malic acid purchased from Schwarz/Mann (the source of malate for this work) was compared with a sample of this compound after chromatographic purification (cf. Methods) as well as with commercial L-malic acid and its monosodium salt from Sigma Chemical Co. Kinetic assays were performed at malate concentrations of 0.67 mM (4 mM $MnCl_2$) and 10 mM (0.1 mM $MnCl_2$) as described under Methods at pH 7.0. The resultant malic enzyme activities using the three malate preparations were identical within experimental error, and the extent of inhibition at the high malate level was 77–81%.

The apparent activation constants of Mn^{2+}, at low $MnCl_2$ concentrations, were obtained from the horizontal intercepts of the extrapolated linear segment of inhibited plots in Figure 2A and decreased from 6.7 to 3.2 μM with increasing malate from 0.5 to 7 mM. A replot of $1/K_{A,app}$ vs. malate concentrations was linear, and extrapolation to zero malate yielded a limiting value (K_A) of 10 μM. The average for two enzyme preparations was 9 μM (Table I) which was consistent with the average K_A of 24 μM determined under noninhibitory conditions (Figure 1) and corresponded with the binding of Mn^{2+} ($K_D \simeq 8$ μM) at the two tight metal sites as determined by direct binding experiments (Hsu et al., 1976).

An enlarged view of Figure 2A at high Mn^{2+} concentrations is shown in Figure 2B. The competitive pattern indicates that increasing Mn^{2+} decreased malate inhibition, causing its elimination at infinite Mn^{2+}. Furthermore, the deinhibited maximal velocity ($\bar{V}'_m$), obtained from the vertical intercept of this pattern, approached (but did not exceed) the uninhibited maximal velocity ($\bar{V}_m$, Table I), as indicated by a $\bar{V}'_m/\bar{V}_m$ ratio of 0.82 calculated for enzyme preparation 1 (0.68 for preparation 2). The apparent activation constant of Mn^{2+} at high Mn^{2+} increased with increasing malate and was 1.22, 2.7, 4.2, and 5.7 mM, respectively, at malate concentrations of 1, 3, 5, and 7 mM. Extrapolation of a linear plot of these constants against malate to zero malate concentration yielded a limiting value (K_A') of 0.48 mM (0.80 mM for preparation 2, Table I) for the second set of Mn^{2+} sites. This value is in good agreement with a dissociation constant of $\simeq$0.9 mM for weak metal sites previously determined from equilibrium binding studies (Hsu et al., 1976). In a separate experiment, data points obtained at malate levels preadjusted to give a "constant" free malate concentration yielded a similar competitive plot (Figure 2C). The $\bar{V}'_m/\bar{V}_m$ ratios (calculated from values in Table I) for the two preparations were 0.56 and 0.66. These results indicate that the observed deinhibitory effect of Mn^{2+} was not an artifact of Mn^{2+}–malate chelate formation.

The apparent inhibition constant of malate (K_i) was estimated from a replot of the vertical intercepts [reciprocal of apparent maximal velocity ($\bar{V}_{m,app}$) at each malate concentration indicated] vs. reciprocal malate concentrations from the primary plots as shown in Figure 2A. Such a plot for preparation 2 is shown in Figure 3. At low malate (<100 μM) the plot was linear, showing Michaelian behavior. The plot then curved upward, in response to increasing malate concentration, as the result of substrate inhibition. The K_m, V_m, and K_i values, obtained from graphic analysis of this plot and an analogous plot from preparation 1, are given in Table

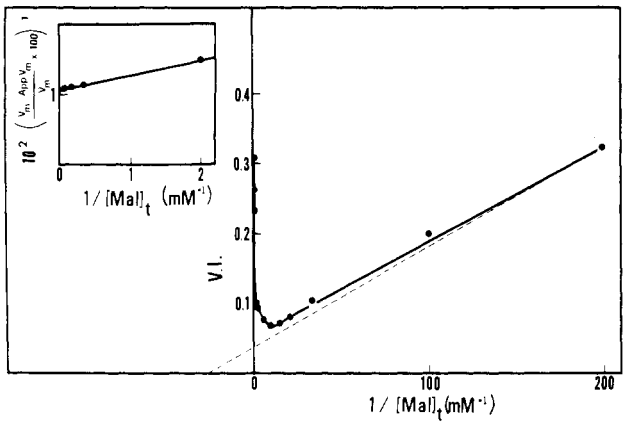

FIGURE 3: Replot of vertical intercept vs. reciprocal malate concentration. The kinetic experiments were carried out as indicated in Figure 2A using malic enzyme preparation 2. This experiment contained more observations at malate concentrations near the crossover point of inhibition than the analogous plot from preparation 1 and was chosen to illustrate more details. The vertical intercepts (reciprocal of $\bar{V}_{m,app}$ at each malate concentration) at inhibitory malate concentrations were obtained by extrapolating linear portions of the plots to infinite Mn^{2+}. The kinetic constants K_m, $\bar{V}_m$, and K_i (malate) were obtained graphically (Cleland, 1970) according to $1/\bar{V}_{m,app} = (K_m/\bar{V}_m)(1/[M]) + (1/\bar{V}_m)(1 + [M]/K_i)$. The dashed line represents the asymptote obtained from this graphic analysis. Inset: double-reciprocal plot of percent inhibition vs. malate concentration.

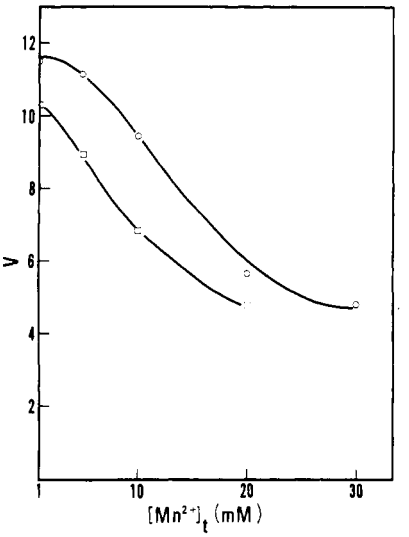

FIGURE 4: Inhibition by $MnCl_2$ at low malate concentrations. The kinetic assays were performed as described in Figure 1 at malate concentrations of (□) 40 and (○) 50 μM and at the $MnCl_2$ concentrations indicated.

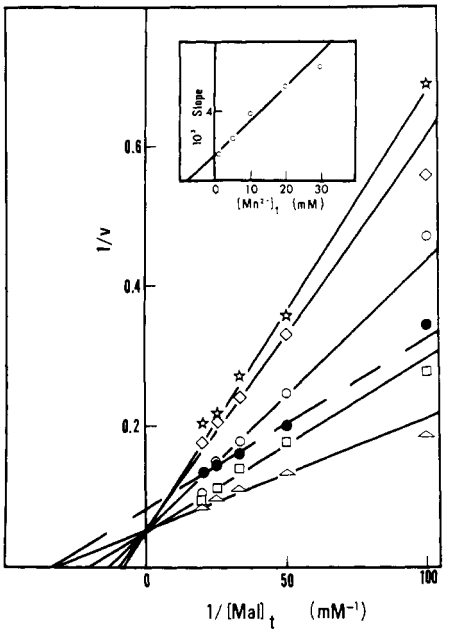

FIGURE 5: Double-reciprocal plots of Mn^{2+} inhibition at noninhibitory malate concentrations. The kinetic assays were performed as described in Figure 1 at the malate concentrations indicated and at $MnCl_2$ concentrations of (△) 1, (□) 5, (○) 10, (◇) 20, and (☆) 30 mM. A plot obtained at subsaturating $MnCl_2$ [(●) 0.1 mM] is shown for comparison. Inset: slope replot.

I together with other kinetic constants. The K_m (average 55 μM) agrees with the value calculated from the uninhibited plots (average 53 μM, Figure 1).

Since $\bar{V}_m$ was obtained with Mn^{2+} saturating only the tight metal sites and was higher than $\bar{V}'_m$, the deinhibited maximal velocity with Mn^{2+} saturating both tight and weak metal sites, it may be concluded that malic enzyme is "half-sited" with respect to Mn^{2+}, i.e., maximally active with Mn^{2+} binding to two sites on the enzyme tetramer.

In a previous report, a plot of $1/v$ vs. free malate concentration at 0.2 or 1 mM fixed free Mn^{2+} (Reynolds et al., 1978; Figure 6A) showed that the velocity fell to a low, but constant level at high malate concentrations, indicating partial and hyperbolic inhibition. In these experiments, the maximum inhibition obtained with Mn^{2+} occupying tight sites only may be determined from a double-reciprocal plot of percent inhibition vs. malate as shown in the Figure 3 inset. Such a determination yielded a value of 93% at infinite malate concentration, confirming the "partial" nature of this inhibition.

Inhibition by Manganese. High concentrations of $MnCl_2$ (>1 mM) were found to inhibit malic enzyme activity at low (noninhibitory) concentrations of malate as shown in Figure 4. Results of a more detailed experiment employing Mn^{2+} at varied inhibitory concentrations, at fixed-changing concentrations of low malate, are illustrated as a double-reciprocal plot in Figure 5. A competitive inhibition pattern was observed, indicating that the inhibitory effect was overcome by saturation with malate at its high-affinity sites. For comparison, a control plot (dashed line) obtained at subsaturating Mn^{2+} is also included. The apparent K_m (K_m of malate at the indicated Mn^{2+} concentration, obtained from horizontal intercepts of plots in Figure 5) increased with increasing Mn^{2+} and was 29, 41, 63, 110, and 126 μM at Mn^{2+} concentrations of 1, 5, 10, 20, and 30 mM. A plot of $K_{m,app}$ against Mn^{2+} concentration yielded a limiting K_m of 28 μM at low Mn^{2+} concentration. This value is somewhat low but consistent with those found in other experiments (Table I).

The inhibition constant of Mn^{2+} (K_i^m), determined from the horizontal intercept of a slope replot (Figure 5 inset) of the competitive inhibition pattern, was found to be 10 ± 2 mM from an average of two separate experiments.

Since Mn^{2+} inhibition was observed only at low ($\leq K_m$) malate, the most plausible explanation for this behavior appears to be that free malate (rather than the Mn^{2+}–malate complex) is the active substrate and that Mn^{2+} inhibits by lowering free malate concentration through formation of the chelation complex. It follows then that the experimentally determined K_i^m represents an estimate of the dissociation constant of this complex. The value of 10 ± 2 mM is in reasonable agreement with the dissociation constant of the Mn^{2+}–malate complex (20 mM) determined by EPR titrations (Hsu et al., 1976). However, other possibilities such as (a) inhibition by Mn^{2+} or (b) inhibition by Mn^{2+}–malate chelate must be considered. This was tested by a replot of Figure 5

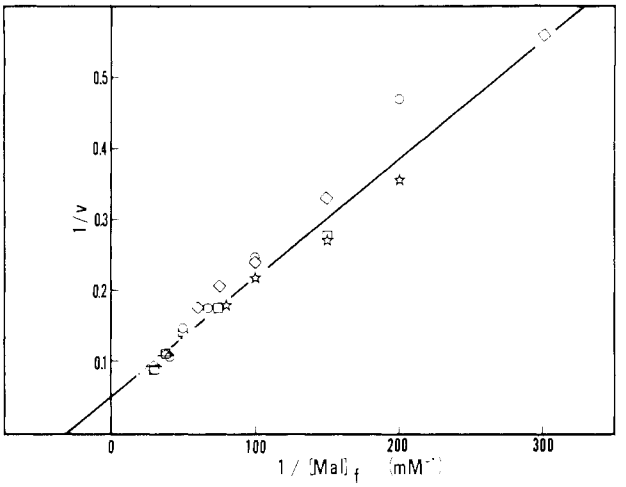

FIGURE 6: Double-reciprocal plot of velocity vs. free malate concentration. Data points were those from Figure 5. Free malate concentrations were calculated by correcting for the Mn^{2+}–malate complex assuming a K_D of 10 mM (Figure 5, inset).

using malate concentrations corrected for the Mn^{2+}–malate complex as shown in Figure 6. The experimental points obtained at the different Mn^{2+} concentrations can now be described by a single linear plot, indicating that the reaction rate is a Michaelian saturation function of free malate levels despite large variations in the concentrations of both Mn^{2+} and Mn^{2+}–malate. This analysis confirms our interpretation that free malate, rather than Mn^{2+}–malate, is the active substrate of malic enzyme. Analyses of Mg^{2+} inhibition patterns on bovine heart fructose-1,6-bisphosphatase (Marcus et al., 1973) and phosphoglucomutase (Ray & Roscelli, 1966; Ray et al., 1966), by this method, have led to the same conclusion regarding the nature of the active substrate.

Molecular Weight of Malic Enzyme at Concentrations Used for Kinetic Assays. In our studies, a precise knowledge of the polymerization state of the enzyme is essential for the interpretation of binding and kinetic data. Direct binding experiments were generally carried out at enzyme concentrations equal to or above those (2–4 μM) used in determining its molecular weight of 260 000 by the equilibrium sedimentation technique (Nevaldine et al., 1974); therefore, the enzyme was presumed to exist in the undissociated, tetrameric state under these conditions. The malic enzyme concentrations used in kinetic assays were much lower, however, and in the range of 1–20 nM.

A gel filtration experiment was performed to determine the molecular size of this enzyme at high dilution in the presence of substrates. In this experiment, 1 mL of 19 nM malic enzyme eluted as a single peak containing 91% of the original activity (final concentration $\simeq$ 4 nM), approximately midway between γ-globulin (M_r 160 000) and apoferritin (M_r 480 000). This result indicates that under these conditions simulating kinetic assays, the enzyme exists as the undissociated tetramer. The presence of substrates was not required for the maintenance of this structure, since the elution volume of malic enzyme was essentially unchanged in a separate experiment without substrates.

Discussion

Steady-state kinetic experiments performed in this study detected the presence of two types of malate sites on malic enzyme on the basis of affinity. These sites are functionally distinct, with the high-affinity (K_m) sites assuming a catalytic role and the low-affinity (K_i) sites inhibiting the former upon occupancy by malate (but not Mn^{2+}). Since a total of four

Scheme I

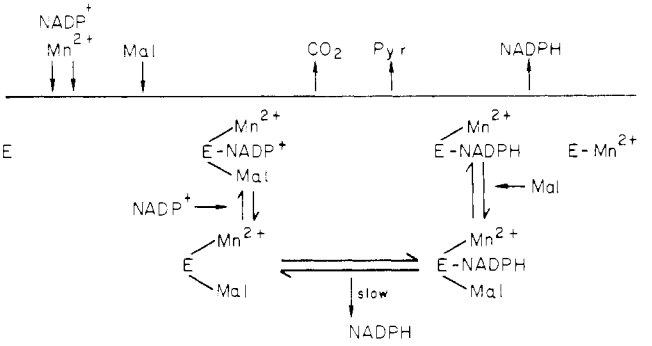

malate sites per enzyme tetramer (one per subunit), consisting of two with tight affinity and two with weak affinity, are detectable by equilibrium binding studies (Pry & Hsu, 1980), it may be reasoned that only the tight sites are involved in catalysis, i.e., half-of-the-sites reactivity of malate. This notion is also supported by the reasonable consistency of K_m (47–63 μM) and K_i (182–270 μM, Table I) with the respective equilibrium dissociation constants K_1 (22–23 μM) and K_2 (350–400 μM) (Pry & Hsu, 1980), notwithstanding differences in the nucleotide present ($NADP^+$ for kinetics, NADPH for direct binding) and that the kinetic parameters may not yield quantitative estimates of the equilibrium values. Given the half-of-the-sites reactivity of Mn^{2+} (cf. Results), the maximal velocity ($\bar{V}_m$) is attained with $NADP^+$ saturating all the enzyme sites and Mn^{2+} and malate saturating only half (or the tight) of these sites. Binding of malate at the two weak sites inhibits the reaction of the "tightly bound" malate. Binding of Mn^{2+} at the weak sites causes deinhibition but has no effect in the absence of "weakly bound" malate (Figure 1).

Inhibition by high substrate concentration has been observed for a number of dehydrogenases (Dalziel, 1975), usually as the result of abortive complex formation. Such a simple mechanism for malate inhibition is shown in Scheme I.

In this scheme, free malate rather than Mn^{2+}–malate is depicted as the active substrate (Figure 6). The existence of the abortive E–Mn^{2+}–NADPH–malate complex has been established in previous studies (Hsu & Lardy, 1967a,b; Reynolds et al., 1978; Pry & Hsu, 1980). This mechanism is consistent with the independent binding of Mn^{2+} and $NADP^+$ (Pry & Hsu, 1980) and with the preferentially ordered sequence between the binding of $NADP^+$ and malate and the release of CO_2, pyruvate, and NADPH (Hsu et al., 1967). At inhibitory levels, malate may react with $NADP^+$ in an alternate minor pathway as shown. Ordered binding of Mn^{2+} and malate (with Mn^{2+} first) is shown by direct binding experiments (Pry & Hsu, 1980) and is supported by the observed uncompetitive nature of malate inhibition (Figure 2). However, since substrate inhibition results from binding of malate at the two weak sites not undergoing catalysis, the actual mechanism must be more complex and involve interactions between adjacent subunits.

Since NADPH release is the rate-limiting step at neutral pH and malate inhibits by depressing NADPH release (Pry & Hsu, 1980), the measured overall rate then gives a quantitative estimate of the "off" constant of this nucleotide. Its "on" constant, which is unchanged, as has been demonstrated for NADH in unproductive enzyme-reduced substrate-reduced nucleotide ternary complexes of simple dehydrogenases (Theorell & McKinley-McKee, 1961; Dickinson & Monger, 1973), may be estimated according to

$$K_{off} = \bar{V} \qquad K_{on} = K_{off}/K_D$$

Scheme II: Active and Inhibited Malic Enzyme Complexes[a]

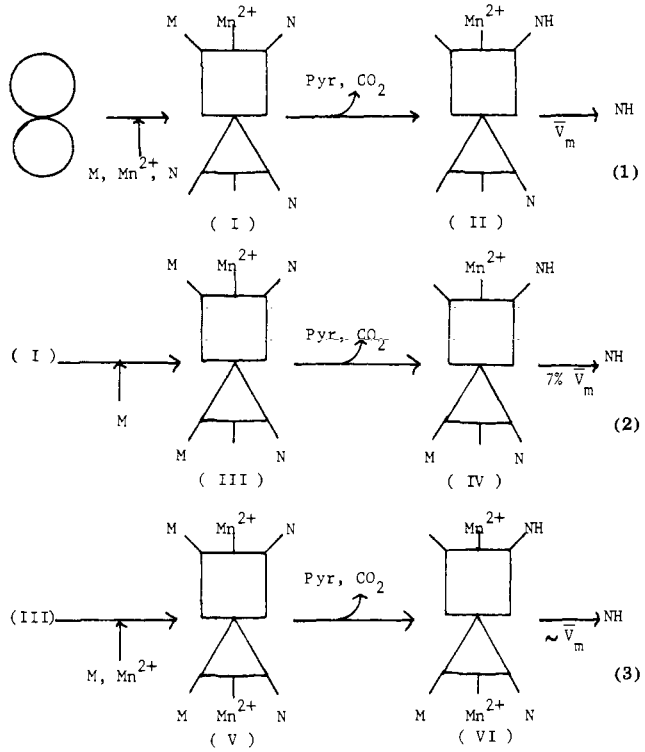

[a] N, Pyr, and M denote $NADP^+$, pyruvate, and malate, respectively. The subunits of the unliganded enzyme (circles) are identical, as judged by their molecular size (Nevaldine et al., 1974), by the reactivity of SH groups (Pry & Hsu, 1978), and by their nucleotide binding behavior (Pry & Hsu, 1980).

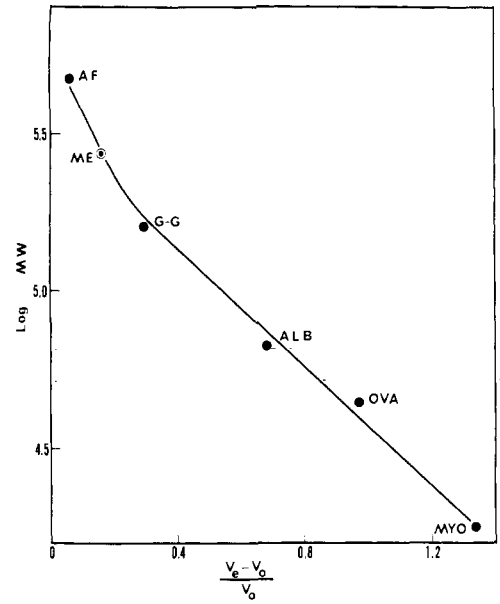

FIGURE 7: Sephadex G-200 column chromatography of malic enzyme at low protein concentration. The Sephadex G-200 column (1.5 × 100 cm) was equilibrated and eluted with 50 mM TEA-HCl buffer, pH 7.4, containing 0.3 mM $NADP^+$, 2 mM $MnCl_2$, and 0.3 mM malate (T = 26 °C). The column was calibrated with 2 mg (in 1.0 mL) of each of the following molecular weight standards from Mann Research: myoglobin (MYO; 17 800); ovalbumin (OVA; 45 000); albumin (ALB; 67 000); γ-globulin (G-G; 160 000); apoferritin (AF; 480 000). Malic enzyme (ME), which had previously been dialyzed against buffer alone, was applied at low concentration (5 μg in 1.0 mL). Elution was effected by descending chromatography at a flow rate of 40 mL/h, regulated with a Buchler peristaltic pump. 3.0-mL fractions were collected and monitored by 280-nm absorption (standards) or enzymatic assays (malic enzyme). V_0 is the void volume estimated with Blue Dextran 2000. V_e is the elution volume of each protein tested.

where $\bar{V}$ is expressed in terms of molecules of substrate converted per second per active site. By use of a maximal velocity ($\bar{V}_m$, Table I) of 59 μmol of NADPH formed per min per mg of enzyme for the fully active preparation 1 and a NADPH dissociation constant of 1.1 μM (Pry & Hsu, 1980), the K_{off} and K_{on} values are found to be 128 s^{-1} and 116 s^{-1} μM^{-1}, respectively, for two active sites per tetramer. These values are reduced by half if all four subunits are simultaneously active.

A possible model showing active and inhibited kinetic complexes is given in Scheme II. In this scheme, a single dimer of a dimer-of-dimers structure is shown. We have established that at low protein concentration (≃4 nM) malic enzyme exists as a tetramer (Figure 7), thus excluding dissociation as a possible cause of heterogeneous binding in the kinetic assays. Each subunit is shown to contain a complete active site capable of binding all reactants. Mn^{2+} and malate bind anticooperatively to the tight (square) and weak (triangle) sites, in contrast to $NADP^+$ which binds equivalently to both sites. In Scheme II, the $NADP^+$ complexes I, III, and V correspond to the NADPH complexes III, IV, and V, respectively, shown in Scheme II of the preceding paper (Pry & Hsu, 1980). Equation 1 depicts the reaction of the fully active quaternary complex (I), with only half of the sites simultaneously undergoing catalysis. Our previous finding (Reynolds et al., 1978) that the transient burst of enzyme-bound NADPH equals approximately half of the active sites supports this analysis. Binding of Mn^{2+} at the weak sites on I has no effect on the catalytic rate. Equation 2 depicts the reaction of the inhibited complex (III) with malate (but not Mn^{2+}) binding at the weak sites, promoting a low conformational change (Reynolds et al., 1978) and depressing NADPH release from the adjoining active site. Binding of Mn^{2+} at the weak site (complex V in eq 3) prevents this change by direct interaction with weakly bound malate, thus relieving this inhibition. The alternate possibility that Mn^{2+} deinhibits by chelation and removal of inhibiting malate has been ruled out by our experiments (Figure 2C).

This model represents a working hypothesis consistent with the unusual binding and kinetic properties of this enzyme and implicates the involvement of subunit interactions in the catalytic mechanism. In this work, we have reasonably, but perhaps not conclusively, eliminated the possible presence of preexisting asymmetric active sites. An experiment is currently under way to determine the identity (or nonidentity) in the primary structure of the four subunits by preparing an enzyme derivative with [^{14}C]bromopyruvate labeling the two tight sites and [^{3}H]-*N*-ethylmaleimide labeling the two weak sites by existing methodology (Pry & Hsu, 1978) and analysis of the amino acid composition and sequence of the radioactive peptides after proteolytic cleavage.

If we assume that the enzyme sites are initially identical, it seems likely that they function alternately during each catalytic cycle in a reciprocating mechanism such as that proposed for a number of polymeric enzymes (Harada & Wolfe, 1968; Lazdunski, 1972, 1974; Mueggler & Wolfe, 1978; Kayalar et al., 1977). For malic enzyme, the noncatalytic sites assume a transient regulatory role, responsible for attenuation of enzyme activity through inhibition by high malate and deinhibition by high Mn^{2+}. Such a conceptually novel mechanism is difficult to test. However, isotope-exchange studies and additional transient and steady-state kinetic experiments would provide more detailed information. A more

conventional, but perhaps less plausible, explanation involving an "allosteric" mechanism such as that proposed for the substrate inhibition of fructose-1,6-bisphosphatase (Marcus et al., 1973) or malate activation of mitochondrial malate dehydrogenase through binding of malate at a "distinct" regulatory site (Telegdi et al., 1973) must also be considered.

Under in vivo conditions Mg^{2+}, rather than Mn^{2+}, is likely to be the predominant activator of malic enzyme. The observed negative cooperativity and half-of-the-sites reactivity, however, is not an artifact observable solely with Mn^{2+} or malate in the presence of Mn^{2+} since both bromopyruvate (Pry & Hsu, 1978) and oxalate (Pry & Hsu, 1980) exhibit half-of-the-sites stoichiometry of binding without the participation of Mn^{2+}. Moreover, preliminary studies on the Mg^{2+}-activated reaction showed that at 2 mM $MgCl_2$, malate inhibition is apparent at 0.5 mM and is relieved at higher Mg^{2+} levels (Liu and Hsu, unpublished results). The latter finding explains the failure by Schimerlik et al. (1977) to detect inhibition with up to 0.5 M malate in the presence of 20 mM Mg^{2+}. The physiological significance of half-of-the-sites reactivity or of malate inhibition is not certain, although these behaviors are coordinated, permitting possible regulation by fluctuations in the cellular concentrations of malate and/or metal cofactors. For this purpose, experiments are currently under way to determine the effects of variations in malate at low Mn^{2+} (≤ 10 μM) and high Mg^{2+} (~ 1 mM) concentrations and high NADPH/$NADP^+$ ratios (Veech et al., 1969) found under a variety of nutritional conditions on malic enzyme activity.

Acknowledgments

The authors are indebted to Dr. W. W. Cleland at the Biochemistry Department, University of Wisconsin, Madison, WI, and Dr. Albert S. Mildvan at the Institute for Cancer Research, Philadelphia, PA, for reviewing the manuscript and offering constructive suggestions on the interpretation of some of our results before publication.

References

Cleland, W. W. (1963a) *Biochim. Biophys. Acta 67*, 104–137.
Cleland, W. W. (1963b) *Nature (London) 198*, 463–465.
Cleland, W. W. (1970) *Enzymes, 3rd Ed. 2*, 1–65.
Dalziel, K. (1975) *Enzymes, 3rd Ed. 11*, 1–60.
Dickinson, F. M., & Monger, G. P. (1973) *Biochem. J. 131*, 261–270.
Harada, K., & Wolfe, R. G. (1968) *J. Biol. Chem. 243*, 4131–4137.
Hsu, R. Y., & Lardy, H. A. (1967a) *J. Biol. Chem. 242*, 520–526.
Hsu, R. Y., & Lardy, H. A. (1967b) *J. Biol. Chem. 242*, 527–532.
Hsu, R. Y., & Pry, T. A. (1979) *Abstracts for 11th International Congress of Biochemistry*, p 293.
Hsu, R. Y., Lardy, H. A., & Cleland, W. W. (1967) *J. Biol. Chem. 242*, 5315–5322.
Hsu, R. Y., Mildvan, A. S., Chang, G. G., & Fung, C. H. (1976) *J. Biol. Chem. 251*, 6574–6583.
Kayalar, C., Rosing, J., & Boyer, P. D. (1977) *J. Biol. Chem. 252*, 2486–2491.
Lazdunski, M. (1972) *Curr. Top. Cell. Regul. 6*, 267–310.
Lazdunski, M. (1974) *Prog. Bioorg. Chem. 3*, 81–140.
Marcus, C. J., Geller, A. M., & Byrne, W. L. (1973) *J. Biol. Chem. 248*, 8567–8573.
Mueggler, P. A., & Wolfe, R. G. (1978) *Biochemistry 17*, 4615–4620.
Nevaldine, B. H., Bassel, A. R., & Hsu, R. Y. (1974) *Biochim. Biophys. Acta 336*, 283–293.
Pry, T. A., & Hsu, R. Y. (1978) *Biochemistry 17*, 4024–4029.
Pry, T. A., & Hsu, R. Y. (1980) *Biochemistry* (preceding paper in this issue).
Ray, W. J., & Roscelli, G. A. (1966) *J. Biol. Chem. 241*, 2596–2602.
Ray, W. J., Roscelli, G. A., & Kirkpatrick, D. S. (1966) *J. Biol. Chem. 241*, 2603–2610.
Reynolds, C. H., Hsu, R. Y., Matthews, B., Pry, T. A., & Dalziel, K. (1978) *Arch. Biochem. Biophys. 189*, 309–316.
Schimerlik, M. I., Grimshaw, C. E., & Cleland, W. W. (1977) *Biochemistry 16*, 571–576.
Telegdi, M., Wolfe, D. V., & Wolfe, R. G. (1973) *J. Biol. Chem. 248*, 6484–6489.
Theorell, H., & McKinley-McKee, J. S. (1961) *Acta Chem. Scand. 15*, 1834–1865.
Veech, R. L., Eggleston, L. V., & Krebs, H. A. (1969) *Biochem. J. 115*, 609–619.
Wilkinson, G. N. (1961) *Biochem. J. 80*, 324–332.